ELSEVIER

Cardiovascular Pathology 18 (2009) 323 – 331

CARDIOVASCULAR PATHOLOGY

Original Article

The effects of NK4 on viral myocarditis mice

Difei Shen[a], Qizhu Tang[a,*], Zhengrong Huang[b], Ying Chen[c], Ran Xiong[a], Hui Wu[a], Ji Huang[a], Siting Feng[a], Ling Yan[a], Zhouyan Bian[a]

[a]*Department of Cardiology, Renmin Hospital, Wuhan University, JieFang Road 238, Wuhan 430060, P.R. China*
[b]*Department of Cardiology, The First Hospital of Xiamen, Xiamen 361003, P.R. China*
[c]*Pediatric Department, Maternal and Child Health Hospital of Hubei, Wuhan 430070, P.R. China*

Received 16 December 2007; received in revised form 11 August 2008; accepted 21 October 2008

Abstract

NK4 may be a promising agent to inhibit tumor invasion and metastasis. To observe the effects of NK4 on the cardiovascular system with pathological injury and to discuss the mechanism, we established an experimental model of viral myocarditis (VCM) by coxsackievirus B3 infection in Balb/c mice on Day 0 and administered NK4 twice daily to the VCM and control mice from Day 20 to Day 45. We then evaluated the cardiac function by means of ultrasonic inspection. Hepatocyte growth factor, TNF (tumor necrosis factor)-α, and angiotensin II levels in the myocardial tissue were measured with enzyme-linked immunosorbent assay. Myocardium histopathology was examined with hematoxylin and eosin stain. Collagen deposition of the myocardium was detected through Masson staining. Microvessel staining with the RECA antibody and apoptosis detection with terminal deoxynucleotidyl transferase-mediated dUTP-biotin end labeling were performed in the myocardium. The changes in MMP3 (matrix metalloproteinase 3), MMP9, TIMP1 (tissue inhibitor of metalloproteinase 1), and TGF (transforming growth factor)-β1 expression in the myocardium were measured by reverse-transcriptase polymerase chain reaction. We found that NK4 intervention increased TGF-β and angiotensin II expression, suppressed MMPs, improved the activities of TIMPs, and then promoted collagen deposition in the myocardium. NK4 intervention also decreased the microvessels' density and increased the apoptotic cell count in the myocardia of VCM mice. However, we did not observe the obvious changes in the myocardia of control mice after NK4 intervention. These data suggest that NK4 made negative impacts on the restoration of cardiac function and the recovery from VCM in the experimental mice.

Keywords: NK4; Hepatocyte growth factor; Myocarditis

1. Introduction

Hepatocyte growth factor (HGF) is produced in various mesenchymeric cells that respond to tissue injury, and it plays biological and physiological roles in tissue regeneration and development of diseases [1–3]. In malignant tumors, HGF induces invasive, angiogenic, and metastatic responses through the c-Met/HGF receptor tyrosine kinase [4–6]. However, HGF has been proven to be a protector of the cardiovascular system in various areas with angiogenesis, antifibrosis, and antiapoptosis effects [7–9]. As we know, fibrosis and apoptosis are the important pathological changes in a lot of cardiovascular diseases. For example, obvious myocardial cell apoptosis and fibrosis could be observed in the acute and chronic stages of myocarditis [10–12]. In addition, viral invasion of vascular endothelium, causing vascular spasm and thus ischemia and reperfusion injury, has been suggested as a pathogenic mechanism of viral myocarditis (VCM) [13]. HGF treatment could improve heart function and ameliorate the progression of myocarditis [14,15].

NK4 was initially purified from fragments obtained by the digestion of HGF with elastase and found to be a potent inhibitor of HGF. NK4 is composed of the N-terminal hairpin and four kringle domains of HGF. It binds c-Met/HGF receptor but does not induce tyrosine phosphorylation of c-Met, thereby competitively inhibiting the c-Met receptor activation induced by HGF. Studies on cancer treatment with

This study was supported by the State Natural Science Foundation of China.

* Corresponding author. Fax: +86 27 88083385.
E-mail address: qizhutang2006@yahoo.com.cn (Q. Tang).

1054-8807/08/$ – see front matter
doi:10.1016/j.carpath.2008.10.008

Table 1
PCR primers and conditions of internal reference and proteins

	Forward primer	Reverse primer	Anneal temperature (°C)	Product length (bp)
GAPDH	gaaacctgccaagtatgatg	accaggaaatgagcttgagc	55.0	191
MMP3	ggcttcagtaccttcccagg	gcagcaaccaggaataggtt	59.0	356
MMP9	tgggcaaaggcgtcgtga	cacagctctcctgccgagtt	59.2	406
TIMP1	cgaatcaacgagaccaccttat	ccgtccacaaacagtgagtgtca	60.8	370
TGF-β1	cggaagcgcatcgaagccatcc	gcaagcgcagctctgcacgg	59.0	346

NK4 in experimental models have supported that treatment of patients with NK4 might effectively suppress the malignant behavior of a tumor through its bifunctional character as an angiogenesis inhibitor and an HGF antagonist [16–19]. Thus, NK4 may be a promising agent to inhibit tumor invasion and metastasis.

Considering its potent inhibitive ability on HGF, it is then interesting to find out what the effect of NK4 on the cardiovascular system, especially that with pathological injury, is. There has been no research on this area reported yet.

In our experiment, we observed the effect of NK4 on established VCM models; here, we discuss the possible mechanisms underlying it.

2. Methodology

2.1. Virus infection and NK4 intervention

Two hundred male Balb/c mice, 6–8 weeks old, were divided into four groups: (a) In the VCM group, 80 mice were inoculated intraperitoneally with a HeLa cell-passaged stock of coxsackievirus B3 (Woodruff variant, 10^3 PFU) originally obtained from the Wuhan University College of Life Science on Day 0. Tissues of half of the mice were collected on Days 20 and 45. (b) In the NK4/VCM group, 60 mice were inoculated intraperitoneally with 10^3 PFU of coxsackievirus B3 on Day 0 and were administered intraperitoneally twice daily with 1.5 mg/kg/day of recombination human NK4 in saline (originally obtained from the Wuhan University College of Life Science, and the purity of NK4 was 95.3% as determined by SDS-PAGE and protein staining) since Day 20. The tissues were collected on Day 45. (c) In the control group, 40 mice were injected intraperitoneally with phosphate-buffered saline on Day 0, and tissues of half of the mice were collected on Day 20. Then, the remaining mice were intraperitoneally administered twice daily with 1.5 mg/kg/day of bovine serum albumin in saline since Day 20. (d) In the NK4/control group, 20 mice were injected intraperitoneally with phosphate-buffered saline on Day 0 and intraperitoneally administered twice daily with 1.5 mg/kg/day of bovine serum albumin in saline since Day 20. The tissues were collected on Day 45.

In the NK4/VCM group, 28 mice died before Day 20 and 15 mice then died between Days 20 and 45, 3 of which were found with abdominal dropsy. Finally, only 17 mice survived by Day 45; In the VCM group, 31 mice died before Day 20 and 49 mice survived by Day 20. Then, 22 mice were sacrificed for tissue collection and 27 were further observed. Finally, 7 mice died, but none of them was found with abdominal dropsy between Days 20 and 45, and 20 mice survived by Day 45. No mouse died in the control (20 mice survived) and NK4/control (20 mice survived) groups before the tissue collection.

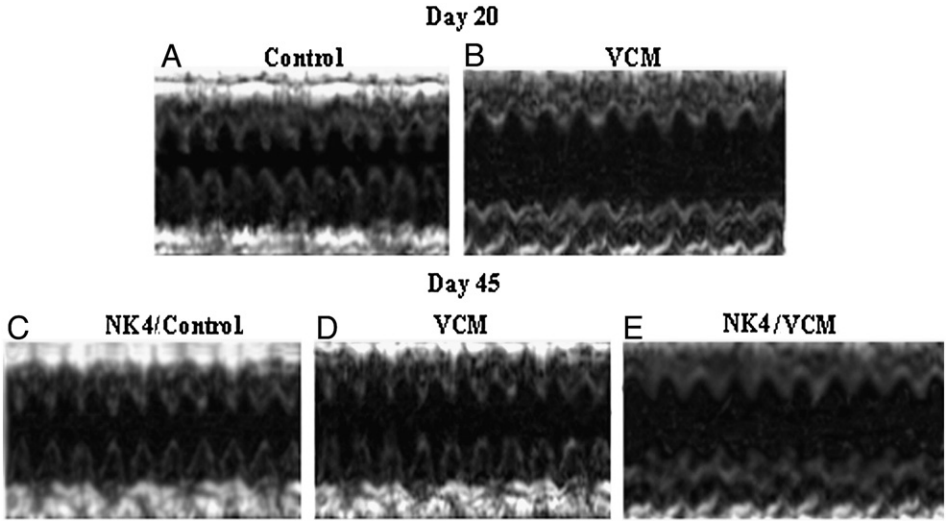

Fig. 1. Echocardiography of mice hearts. Panels (A), (B), (C), (D), and (E) are M-mode echocardiographic recordings of mice from the control group, VCM group (Day 20), NK4/control group (Day 45), VCM group (Day 45), and NK4/VCM group (Day 45), respectively.

Table 2
Morphology and echocardiographic recordings of mice hearts

	Day 20		Day 45			
Parameter	Control (n=20)	VCM (n=22)	Control (n=20)	Control/NK4 (n=20)	VCM (n=20)	VCM/NK4 (n=17)
HW/BW (mg/g)	4.52±0.33 [a]	5.72±0.51 [b]	4.42±0.54 [c]	4.51±0.49 [c]	4.77±0.85	6.13±0.62 [b, d]
V_p (cm/s)	85.77±6.59 [a]	53.93±9.36 [b]	81.59±7.81 [c]	85.02±6.16 [c]	73.25±9.23	62.14±8.26 [b, d]
V_i (cm^2)	3.71±0.36 [a]	2.57±0.41 [b]	3.55±0.35	3.36±0.42	3.04±0.39	2.57±0.48
LVEDD (mm)	4.20±0.31	4.36±0.42	4.34±0.37	4.29±0.41	4.43±0.52	4.63±0.48
LVESD (mm)	2.87±0.21 [a]	3.69±0.27 [b]	2.94±0.35 [c]	3.03±0.32 [c]	3.38±0.44	3.92±0.41 [b, d]
FS (%)	44.33±5.12 [a]	17.39±2.62 [b]	45.92±6.35 [a, c]	39.35±5.73 [c]	33.17±3.77 [b, c]	20.71±4.64 [a, b, d]

HW/BW, heart weight/body weight; V_p, peak velocity of aorta; V_i, flow velocity integral of aorta; FS, fractional shortening; LVEDD, left ventricular end-diastolic dimension; LVESD, left ventricular end-systolic dimension.

[a] Compared with the VCM group, $P<.05$.
[b] Compared with the control group, $P<.05$.
[c] Compared with the NK4/VCM group, $P<.05$.
[d] Compared with the NK4/control group, $P<.05$.

2.2. Morphological and functional changes in mice hearts

Transthoracic echocardiograms of conscious mice were obtained on Days 20 and 45. Peak velocity of aorta, flow velocity integral of aorta, fractional shortening, left ventricular end-diastolic dimension, and left ventricular end-systolic dimension were calculated to evaluate the heart function of mice.

All experiments were performed according to the institutional guidelines for animal care that are in line with the National Institutes of Health's guidelines for the care and use of animals (1996, No. 85-23).

2.3. Pathological and histological examinations

Mice were then sacrificed, and each of the hearts was cut longitudinally in halves, with one half embedded in paraffin and the other frozen in liquid nitrogen and stored at −80°C. Five-micrometer-thick sections from the mice were prepared by a routine procedure to evaluate pathological changes in the hearts. The slices were stained with hematoxylin and eosin (H&E).

Collagen deposition in the myocardium was detected through Masson staining to reflect the extent of fibrosis. Five fields of view were chosen randomly in each section, and the collagen area fraction [Collagen Area Fraction (CAF)=Collagen Area/View Area] was calculated using an Image-Pro Plus image analysis system (Media Cybernetics, USA). The mean CAF was chosen to represent the CAF of each sample.

Microvessels in the myocardium stained with the RECA antibody and their density (microvessels per square millimeter) were measured (usually the LV myocardium) on Day 45. From each mouse, 7 to 10 microscopic high-power fields (×400; total area ranging from 250,000 to 350,000 μm) with transversely sectioned myocytes were digitally recorded using the Image-Pro Plus image analysis system. The microcirculation was defined as vessels beyond the third-order arterioles, with a diameter of 150 μm or less, supplying tissue between arterioles and venules. To correct for differences in LV hypertrophy, we divided microvessel density by LV weights (corrected for body weight).

`Apoptosis detection was performed in the myocardium on Day 45. Terminal deoxynucleotidyl transferase-mediated dUTP-biotin end labeling was performed according to the protocol outlined for the In Situ Cell Death Detection Kit (Jingmei Biotech). Then, sections were counterstained with H&E stain, dehydrated through a graded series of alcohol, and coverslipped for evaluation by light microscopy (×400). Ten-by-ten fields of view were evaluated to count the apoptotic myocardial cells, and the mean was chosen to represent the number of apoptotic myocardial cells in each group.

2.4. Measurement of cytokine level in the myocardium

The heart tissues were homogenized in buffer composed of 20 mM Tris–HCl (pH 7.4), 2 M NaCl, 0.01% Tween 80, 1 mM EDTA, and 1 mM phenylmethylsulfonyl fluoride. The homogenates were centrifuged, and the supernatants served as tissue extracts. HGF and TNF (tumor necrosis factor)-α levels were measured with an enzyme-linked immunosorbent assay using HGF, TNF-α (Jingmei Biotech), and angiotensin (Ang) II (R&D Systems) enzyme-linked immunosorbent assay kits.

2.5. Reverse-transcriptase polymerase chain reaction

Reverse-transcriptase polymerase chain reaction (PCR) was used to detect the transcript levels of proteins in the myocardial tissues of different groups. The PCR primers and the conditions that were used to obtain the MMP3 (matrix metalloproteinase 3), MMP9, TIMP1 (tissue inhibitor of metalloproteinase 1), TGF (transforming growth factor)-β1, and internal reference (GAPDH) sequences are summarized in Table 1.

2.6. Statistical analysis

The data were analyzed by paired t test, and all values are expressed as mean±SEM. The data were considered to be

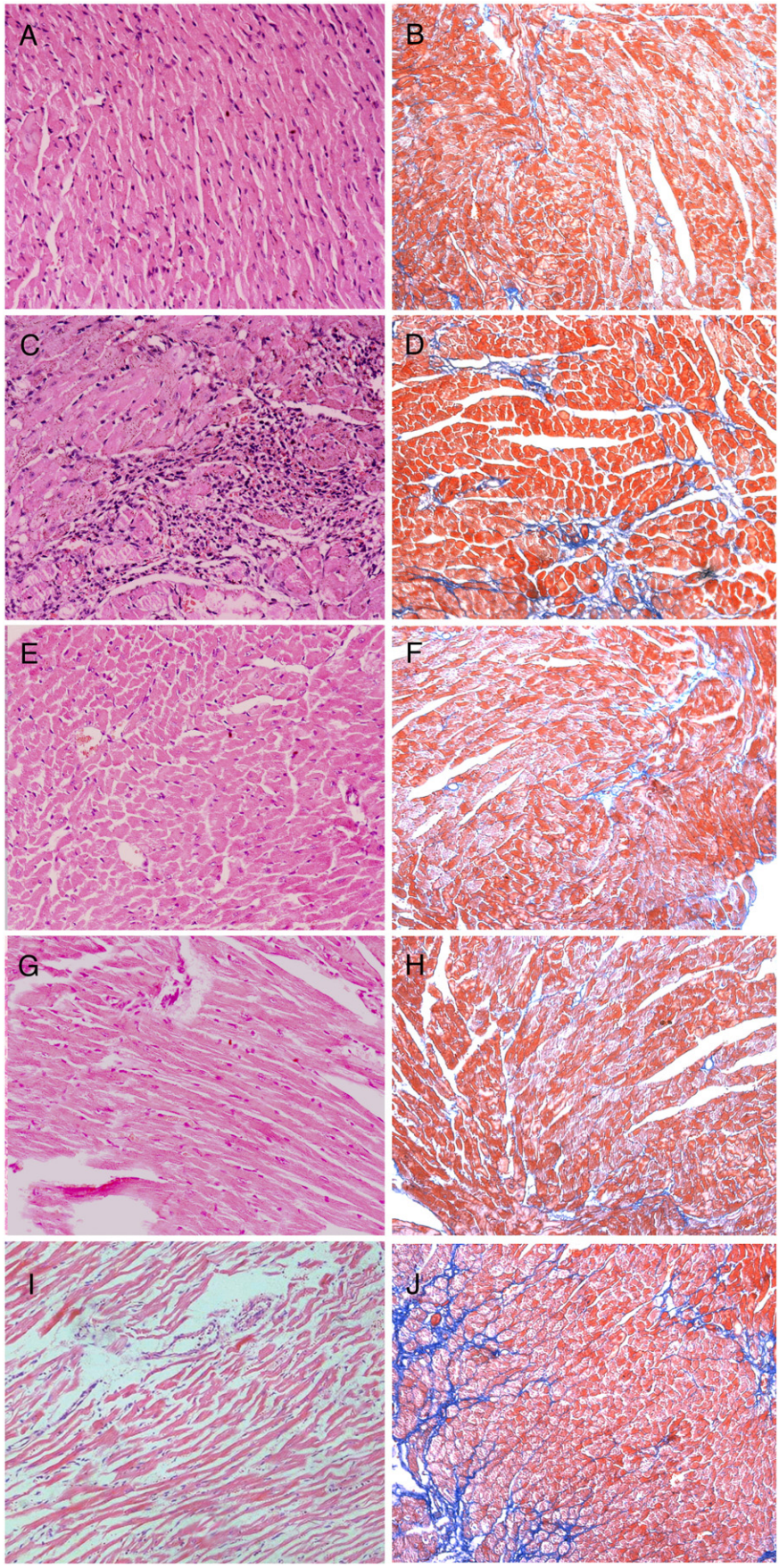
A
B
C
D
E
F
G
H
I
J

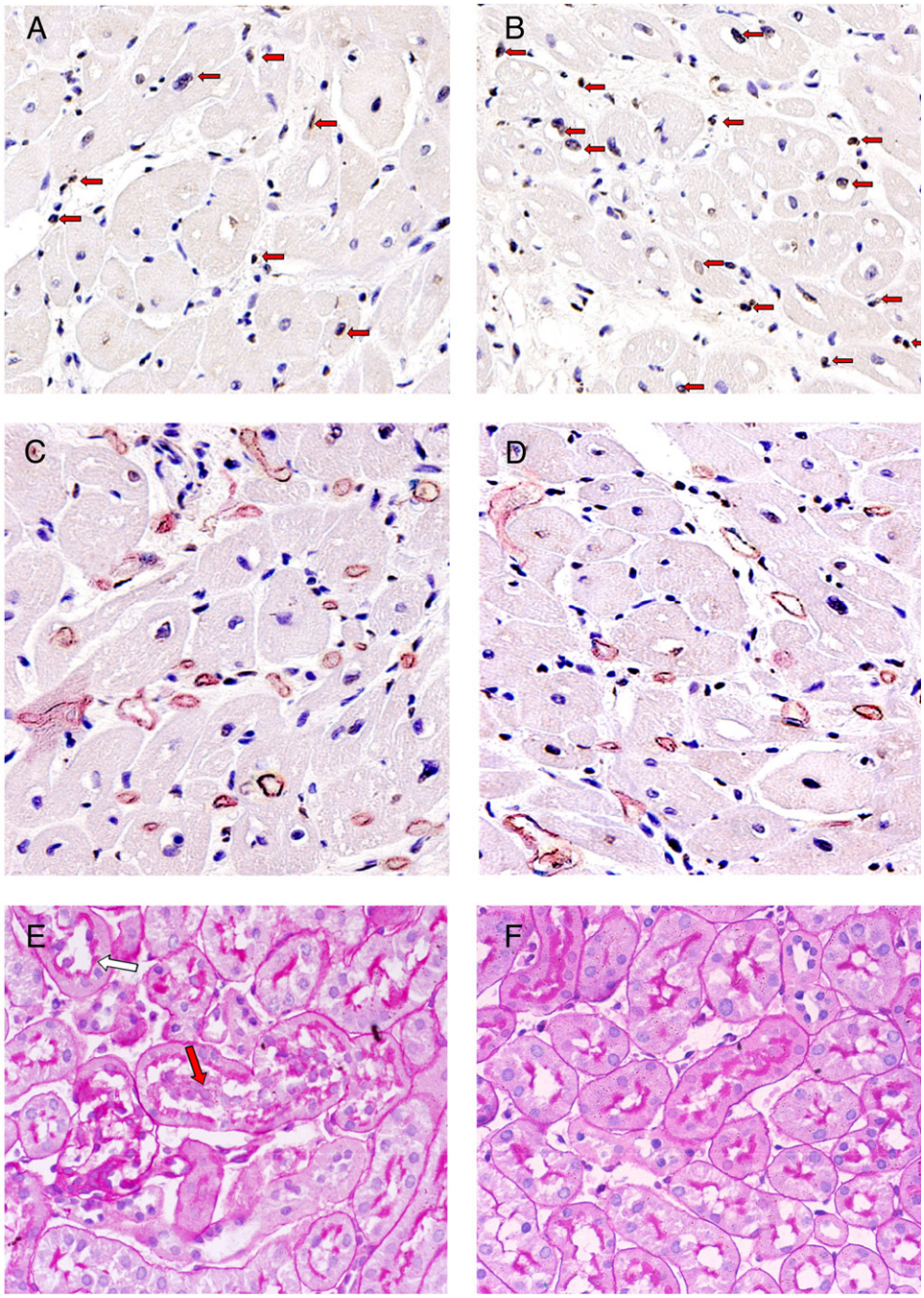

Fig. 3. Apoptotic myocardial cell detection with terminal deoxynucleotidyl transferase-mediated dUTP-biotin end labeling (A and B, original magnification ×400), RECA-antibody stain of microvessels in the myocardium (C and D, original magnification ×400), and light microscopic findings in VCM and control kidneys (E and F) on Day 45. The nucleus of apoptotic cell was stained brown (arrows). The apoptotic cells in NK4/VCM group mice (B) were greater than those in VCM group mice (A). Mice myocardia were stained with the RECA antibody (red), and sections were counterstained with hematoxylin–eosin. The microvessel density in NK4/VCM group mice (D) was lower than that in VCM group mice (C). (E) Renal tubular epithelial cells of certain tubular segments in the NK4/VCM group detached from the tubular basement membrane (red arrow). Bush border of parts of epithelial tubular cells disappeared (white arrow, PAS stain, original magnification ×200). (F) There was no obvious pathological change in the kidneys of VCM group mice (PAS stain, original magnification ×400).

Fig. 2. Pathological and histological changes in mice hearts. Panels (A), (C), (E), (G), and (I) are images of H&E-stained myocardial sections from the control group, VCM group (Day 20), NK4/control group (Day 45), VCM group (Day 45), and NK4/VCM group (Day 45) group, respectively (original magnification ×200). (C) On Day 20, a marked infiltration by mononuclear cells and a massive myocardial necrosis were observed. (E) There was no obvious inflammation and fibrosis in the NK4/control and VCM groups on Day 45. Although there was no obvious inflammation, a certain extent of fibrosis with collagen deposition was observed in the myocardia of NK4/VCM group mice on Day 45. Panels (B), (D), (F), (H), and (J) are images of Masson-stained myocardial sections from the control group, VCM group (Day 20), NK4/control group (Day 45), VCM group (Day 45), and NK4/VCM group (Day 45), respectively (original magnification ×200). The depositing collagens were stained to be blue.

Table 3
Histological and cytokine level changes in mice myocardia

	Day 20		Day 45			
Parameter	Control (n=20)	VCM (n=22)	Control (n=20)	Control/NK4 (n=20)	VCM (n=20)	VCM/NK4 (n=17)
CAF (%)	0.731±0.22 [a]	2.47±0.41 [b]	0.85±0.17 [a, c]	1.21±0.25 [c]	1.72±0.41 [b, c]	6.32±1.31 [a, b, d]
NAC			7.96±1.4 [c]	9.55±2.4 [c]	11.92±3.3 [c]	28.14±6.2 [a, b, d]
MD (microvessels/mm^2)			659±73 [c]	591±82	705±102 [c]	433±62 [a, b]
MHGF (ng/g)	4.76±0.53 [a]	11.22±1.03 [b]	4.58±0.42	4.93±0.72 [c]	5.11±0.48 [c]	3.17±0.55 [a, d]
MTNF-α (ng/g)	10.36±1.51 [a]	17.59±3.31 [b]	9.31±1.87 [c]	9.54±1.02 [c]	12.88±2.54	15.69±2.11 [b, d]
MAng II (ng/g)	0.47±0.05 [a]	0.86±0.15 [b]	0.52±0.06 [c]	0.60±0.09 [c]	0.71±0.08 [c]	1.23±0.16 [a, b, d]

CAF, collagen area fraction; NAC, number of apoptotic cells; MD, microvessel density; MHGF, HGF in the myocardium; MTNF-α, TNF-α in the myocardium; MAng II, angiotensin II in the myocardium.

[a] Compared with the VCM group, $P<.05$.
[b] Compared with the control group, $P<.05$.
[c] Compared with the NK4/VCM group, $P<.05$.
[d] Compared with the NK4/control group, $P<.05$.

significantly different when the two-tailed P value was less than .05.

3. Results

3.1. Heart functional changes

The heart function of the VCM group mice was decreased on Day 20. On Day 45, the heart functions were not different between the control and NK4/control groups, and the heart function of the VCM group mice improved but still lower than that of the control group mice (the difference was not statistically significant). In the NK4/VCM group, the heart function was even lower than that of the VCM group, and the difference was not statistically significant (Fig. 1; Table 2).

3.2. Pathological and histological changes

On Day 20, after inoculation, a marked inflammation of the mice heart was observed. There was no obvious inflammation and fibrosis in the control, NK4/control, and VCM groups, and we did not find significant differences in the microvessels' density and apoptotic cell count among the three groups on Day 45. However, we did observe significant differences between the VCM and NK4/VCM groups: A certain extent of fibrosis with collagen deposition was observed in the myocardia of the NK4/VCM group mice on Day 45. In addition, compared with those in the VCM group, the microvessels' density decreased and the apoptotic cell count increased in the myocardia of the NK4/VCM group mice (Figs. 2 and 3; Table 3).

In addition, we did not find any obvious pathological changes in the livers of all the mice. However, we did find significant nephric tubular injury in the kidneys of mice with abdominal dropsy and in two other mice from the NK4/VCM group, but no obvious pathological change was found in the kidneys of the VCM, control, and NK4/control group mice (Fig. 3).

3.3. Cytokine level in the myocardium

Compared with those in the control group, the HGF, TNF-α, and Ang II levels in the myocardial tissue increased in the VCM group on Day 20 and decreased to the same levels as those in the control group on Day 45. After NK4 intervention, in the NK4/VCM group, the HGF levels in the myocardium were lower ($P<.05$), while the TNF-α and Ang II levels in the myocardium were higher than those in the VCM group (the difference was not statistically significant), but we did not observe any obvious differences in the cytokine levels in the myocardial tissue between the control/NK4 group mice and control group mice on Day 45 (Table 3).

3.4. Expression of remodeling relative protein mRNAs

Compared with those of the control group, on Day 20, MMP3 and MMP9 mRNAs of the VCM group significantly increased, while TIMP1 mRNA decreased. Although MMP3 mRNA expression was greater than that in the control group, TIMP1 mRNA also increased in the VCM group on Day 45. In the NK4/VCM group, MMP3 mRNA expression and MMP9 mRNA expression were less, while TIMP1 mRNA expression was greater than that in the VCM group on Day 45. The TGF-β1 mRNA level in the VCM group increased on Day 20 and was still greater than (no statistical difference) that in the control group on Day 45. However, it did dramatically increase in the NK4/VCM group on Day 45. In the control/NK4 group, the levels of the remodeling relative protein mRNAs mentioned above were close to those in the control group on Day 45 (Fig. 4).

4. Discussion

MMPs belong to a family of proteases that are responsible for degradation of ECM proteins. The activities of MMPs can be specifically inhibited by tissues of an endogenous class of low-molecular-weight molecules called TIMPs [20,21]. MMPs/TIMPs are expressed and activated

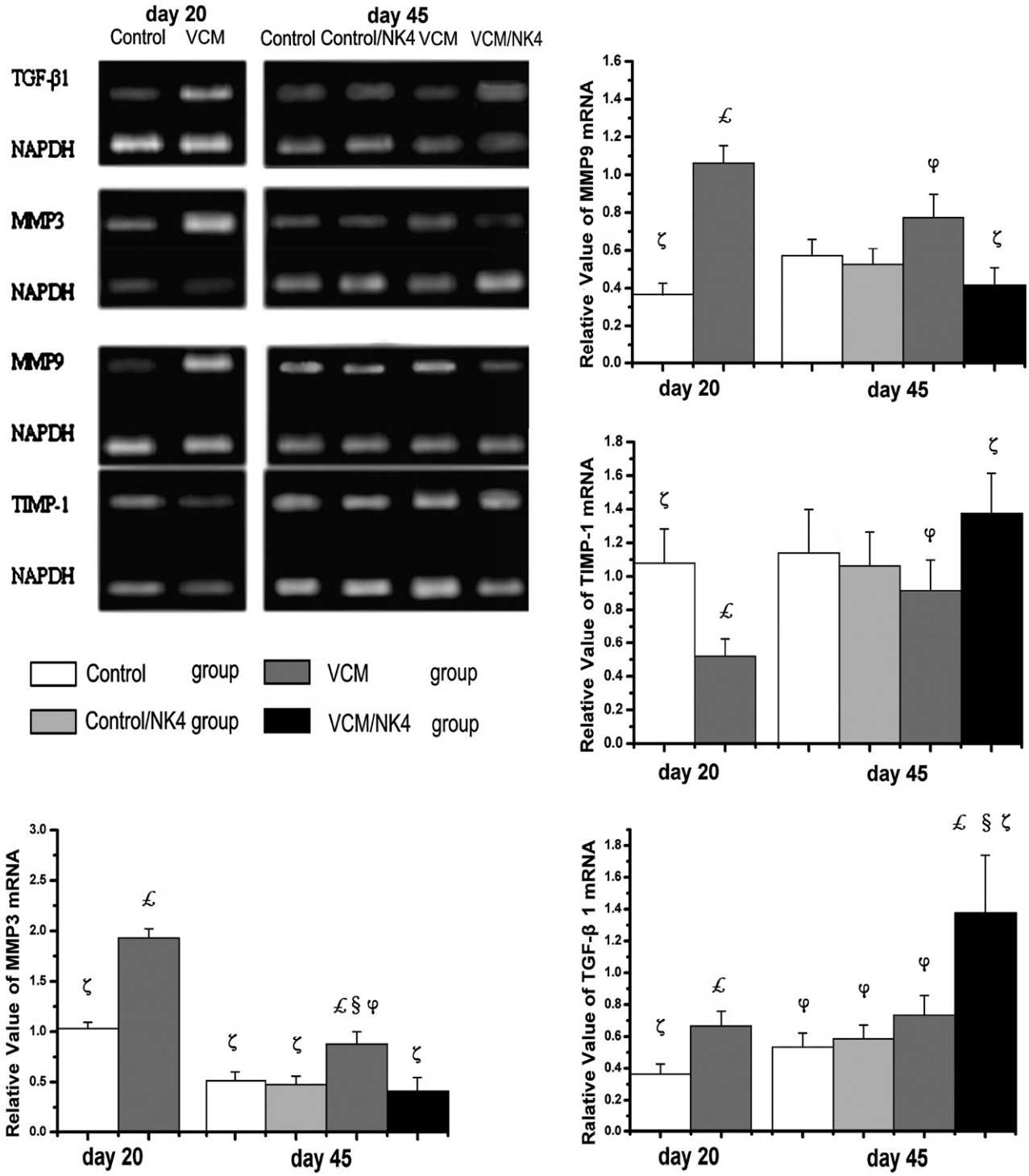

Fig. 4. Semiquantification of TGF-β1, MMP3, MMP9, and TIMP1 mRNA expression in the myocardium by reverse-transcriptase PCR and statistical graphs of relative values of these proteins' mRNA expression. £Compared with the control group, $P<.05$. §Compared with the NK4/control group, $P<.05$. ζCompared with the VCM group, $P<.05$. φCompared with the NK4/VCM group, $P<.05$.

throughout the myocardium in response to local injuries, such as myocardial infarction, and may thus contribute to global changes in collagen abundance, composition, and remodeling of the hearts [22–24].

Various signaling molecules, such as neurohormones, growth factors, and cytokines, have been found to modulate MMP expression and TIMP expression. In particular, proinflammatory cytokines, such as TNF-α, have been implicated in both MMP expression and the reduction of endogenous inhibitors, leading to overall increases in MMP activity [21,22,25]. HGF is a potent activator of MMPs, leading to degradation of collagen type 1 [9,26]. TGF-β is a

key humoral factor for the promotion of tissue fibrosis by increasing the extracellular matrix and TIMP expression while at the same time suppressing MMP activity. TGF-β suppresses HGF expression, and HGF suppresses TGF-β expression [27]. Thus, tissue fibrosis is regulated by a balance in TGF-β and HGF production. Activation of Ang II is also believed to play an important role in the pathogenesis of fibrosis in cardiovascular disease [28–31]. In an ischemic rat heart, locally generated Ang II is correlated to TGF-β1 expression and synthesis [28], suggesting a concerted action of these two factors. It is well documented that the inhibition of Ang II attenuates fibrotic change in the heart in cardiomyopathic hamsters [9,32,33]. In addition, HGF can inhibit Ang II production and attenuate the fibrotic change induced by Ang II [9].

In our experiment, the HGF level in mice myocardia was increased on Day 20. The possible reason is that the elevated levels of proinflammatory cytokines (TNF-α and IL-1β, for example) induced HGF secretion by cardiocyte, endothelial cells, and fibroblast [28] in the heart. Although TGF-β1 and Ang II increased to a certain extent in the myocardia of the VCM mice, in this phase, the proinflammatory cytokines and HGF placed a dominant effect on the MMP/TIMP system and induced an activated situation of ECM digestion to promote the elimination of virus and necrosis tissues and myocardial wound healing. On Day 45, the levels of MMPs/TIMPs and cytokines in the myocardia of VCM group mice were more close to those in the control group mice. It indicated a recovery situation from the acute VCM, although there may still be potential inflammation and ECM remodeling.

However, after the VCM mice received 25 days of NK4 treatment with the same method as that in previous research [34], we found that the expression of HGF and MMPs was suppressed, TGF-β and Ang II increased, and the activities of TIMPs were improved. These changes promoted collagen deposition in the myocardium. In addition, the microvessels' density in the myocardia of the NK4/VCM group mice reduced. It has been reported that NK4 inhibits the angiogenesis mediated by HGF and that the antiangiogenic activity of NK4 seems to be independent of HGF antagonist activity [35,36]. We also found that cell apoptosis increased in the myocardia of NK4 intervention group mice. Possible reasons include the following: (a) the antiapoptotic effect of HGF was suppressed by NK4; (b) the antiangiogenic activity of NK4 reduced the myocardial blood supply from microvessels; and (c) increased inflammatory cytokines (TNF-α, for example) might also increase apoptotic cells.

However, we did not observe these changes in the control/NK4 group after the mice received 25 days of NK4 treatment. It indicated that the expression of HGF was maintained at a low level and that inhibiting this part of HGF would not cause obvious pathological changes in the normal condition.

In addition, we could not ascertain the direct reason of the three cases of abdominal dropsy observed in the NK4 intervention group mice because we did not observe the case with abdominal dropsy in the control/NK4 group. They might have been induced by heart dysfunction and/or renal inadequacy caused by nephric tubular injury. Further research is needed to prove if abdominal dropsy and nephric tubular injury are related to NK4 intervention.

5. Conclusions

In our study, we found that treating the VCM mice with NK4 increased fibrosis and cell apoptosis and decreased microvessels' density in the myocardium. These interfered with the improvement of cardiac function and recovery from VCM in the experimental mice. These indicate that we should pay more attention to the adverse effects of NK4 on the cardiovascular system with pathological injury when it is used as a promising anticancer agent.

References

[1] Zarnegar R, Michalopoulos GK. The many faces of hepatocyte growth factor: from hepatopoiesis to hematopoiesis. J Cell Biol 1995;129:1177–80.
[2] Matsumoto K, Nakamura T. Hepatocyte growth factor (HGF) as a tissue organizer for organogenesis and regeneration. Biochem Biophys Res Commun 1997;239:639–44.
[3] Birchmeier C, Gherardi E. Developmental roles of HGF/SF and its receptor, the c-Met tyrosine kinase. Trends Cell Biol 1998;8:404–10.
[4] Jeffers M, Rong S, Vande Woude GF. Hepatocyte growth factor/scatter factor-Met signaling in tumorigenicity and invasion/metastasis. J Mol Med 1996;74:505–13.
[5] To CT, Tsao MS. The roles of hepatocyte growth factor/scatter factor and Met receptor in human cancers. Oncol Rep 1998;5:1013–24.
[6] Jiang WG, Hiscox S, Matsumoto K, et al. Hepatocyte growth factor/scatter factor, its molecular, cellular and clinical implications in cancer. Crit Rev Oncol Hematol 1999;29:209–48.
[7] Rosen EM, Lamszus K, Laterra J, et al. HGF/SF in angiogenesis. Ciba Found Symp 1997;212:215–29.
[8] Nakamura T, Mizuno S, Matsumoto K, et al. Myocardial protection from ischemia/reperfusion injury by endogenous and exogenous HGF. J Clin Invest 2000;106:1511–9.
[9] Taniyama Y, Morishita R, Nakagami H, et al. Potential contribution of a novel antifibrotic factor, hepatocyte growth factor, to prevention of myocardial fibrosis by angiotensin II blockade in cardiomyopathic hamsters. Circulation 2000;102:246–52.
[10] Saraste A, Arola A, Vuorinen T, et al. Cardiomyocyte apoptosis in experimental coxsackievirus B3 myocarditis. Cardiovasc Pathol 2003;12:255–62.
[11] Colston JT, Chandrasekar B, Freeman GL. Expression of apoptosis-related proteins in experimental coxsackievirus myocarditis. Cardiovasc Res 1998;38:158–68.
[12] Fairweather D, Frisancho-Kiss S, Yusung SA, et al. Interferon-gamma protects against chronic viral myocarditis by reducing mast cell degranulation, fibrosis, and the profibrotic cytokines transforming growth factor-beta 1, interleukin-1 beta, and interleukin-4 in the heart. Am J Pathol 2004;165:1883–94.
[13] Suddaby EC. Viral myocarditis in children. Crit Care Nurse 1996;16:73–82.
[14] Futamatsu H, Suzuki J, Mizuno S, et al. Hepatocyte growth factor ameliorates the progression of experimental autoimmune myocarditis: a potential role for induction of T helper 2 cytokines. Circ Res 2005;96(8):823–30.

[15] Isobe M, Futamatsu H, Suzuki J. Hepatocyte growth factor: effects on immune-mediated heart diseases. Trends Cardiovasc Med 2006;16(6): 188–93.
[16] Matsumoto K, Nakamura T. NK4 (HGF-antagonist/angiogenesis inhibitor) in cancer biology and therapeutics. Cancer Sci 2003;9: 4321–7.
[17] Maemondo M, Narumi K, Saijo Y, et al. Targeting angiogenesis and HGF function using an adenoviral vector expressing the HGF-antagonist NK4 for cancer therapy. Mol Ther 2002;5:177–85.
[18] Hirao S, Yamada Y, Koyama F, et al. Tumor suppression effect using NK4, a molecule acting as an antagonist of HGF, on human gastric carcinomas. Cancer Gene Ther 2002;9:700–7.
[19] Saimura M, Nagai E, Mizumoto K, et al. Intraperitoneal injection of adenovirus-mediated NK4 gene suppresses peritoneal dissemination of pancreatic cancer cell line AsPC-1 in nude mice. Cancer Gene Ther 2002;9:799–806.
[20] He CS, Wilhelm SM, Pentland AP, et al. Tissue cooperation in a proteolytic cascade activating human interstitial collagenase. Proc Natl Acad Sci U S A 1989;86:2632–6.
[21] Li YY, McTiernan CF, Feldman AM. Proinflammatory cytokines regulate tissue inhibitors of metalloproteinases and disintegrin metalloproteinase in cardiac cells. Cardiovasc Res 1999;42:162–72.
[22] Li YY, McTiernan CF, Feldman AM. Interplay of matrix metalloproteinases, tissue inhibitors of metalloproteinases and their regulators in cardiac matrix remodeling. Cardiovasc Res 2000;46:214–24.
[23] Thomas CV, Coker ML, Zellner JL, et al. Increased matrix metalloproteinase activity and selective upregulation in LV myocardium from patients with end-stage dilated cardiomyopathy. Circulation 1998;97:1708–15.
[24] Brauer PR, Cai DH. Expression of tissue inhibitor of metalloproteinases (TIMPs) during early cardiac development. Mech Dev 2002;113: 175–9.
[25] Spinale FG, Coker ML, Krombach SR, et al. Matrix metalloproteinase inhibition during the development of congestive heart failure: effects on left ventricular dimensions and function. Circ Res 1999;85: 364–76.
[26] Fujiuchi Y, Nagakawa O, Murakami K, et al. Effect of hepatocyte growth factor on invasion of prostate cancer cell lines. Oncol Rep 2003;10:1001–6.
[27] Mizuno S, Kurosawa T, Matsumoto K, et al. Hepatocyte growth factor prevents renal fibrosis and dysfunction in a mouse model of chronic renal disease. J Clin Invest 1998;101:1827–34.
[28] Hanatani A, Yoshiyama M, Kim S, et al. Inhibition by angiotensin II type 1 receptor antagonist of cardiac phenotypic modulation after myocardial infarction. J Mol Cell Cardiol 1995;27:1905–14.
[29] Shiota N, Fukamizu A, Takai S, et al. Activation of angiotensin II-forming chymase in the cardiomyopathic hamster heart. J Hypertens 1997;15:431–40.
[30] Danser AH, van-Kesteren CA, Bax WA, et al. Prorenin, renin, angiotensinogen, and angiotensin-converting enzyme in normal and failing human hearts: evidence for renin binding. Circulation 1997;96: 220–6.
[31] Urata H, Boehm KD, Philip A, et al. Cellular localization and regional distribution of an angiotensin II-forming chymase in the heart. J Clin Invest 1993;91:1269–81.
[32] Nakamura F, Nagano M, Kobayashi R, et al. Chronic administration of angiotensin II receptor antagonist, TCV-116, in cardiomyopathic hamsters. Am J Physiol Heart Circ Physiol 1994;267:H2297–304.
[33] Watanabe M, Kawaguchi H, Onozuka H, et al. Chronic effects of enalapril and amlodipine on cardiac remodeling in cardiomyopathic hamster hearts. J Cardiovasc Pharmacol 1998;32:248–59.
[34] Daisaku T, Naoki M, Keiji K, et al. Inhibition of growth, invasion, and metastasis of human pancreatic carcinoma cells by NK4 in an orthotopic mouse model. Cancer Res 2001;61:7518–24.
[35] Kuba K, Matsumoto K, Date K, et al. HGF/NK4, a four-kringle antagonist of hepatocyte growth factor, is an angiogenesis inhibitor that suppresses tumor growth and metastasis in mice. Cancer Res 2000; 606:737–6743.
[36] Kuba K, Matsumoto K, Ohnishi K, et al. Kringle 1–4 of hepatocyte growth factor inhibits proliferation and migration of human microvascular endothelial cells. Biochem Biophys Res Commun 2000;279: 846–52.